International Journal of Automotive Technology, Vol. 20, No. 1, pp. 127–135 (2019)
DOI 10.1007/s12239–019–0012–0

pISSN 1229–9138/ eISSN 1976–3832

MODEL-BASED CONTROL OF ELECTROMAGNETIC VALVE ACTUATORS FOR ENGINE SPEED CONTROL

Huitao Chen, Siqin Chang* and Aimin Fan

School of Mechanical Engineering, Nanjing University of Science and Technology, Nanjing 210094, China

(Received 11 January 2018; Revised 28 July 2018; Accepted 5 August 2018)

ABSTRACT–The introduction of electromagnetic valve actuators (EMVA) benefits engine fuel economy, torque performance and reduction of emissions. Meanwhile, it complicates the controller for the purpose of regulating the additional freedom degrees of intake valvetrain, such as valve lift, opening timing and opening duration. In order to address the control issue of EMVA application, a model-based controller is needed to realize that the cylinder air charge is regulated by controlling the EMVA motion directly for controlling the engine speed and output torque. For the development of the controller, a control-oriented model of engine with EMVA that can simulate the intake process of unthrottled operation, torque generation and crankshaft rotational dynamics was first developed. Then a model-based EMVA controller was designed to regulate the actuation of electromagnetic intake valves which consisted of a feedforward and a PID feedback module. According to torque-based concept, engine speed reference was translated into torque demand using optimal control theory and the speed control problem was solved as two parts: torque management that decided torque demand and the torque demand tracking. The simulations carried out in Matlab/Simulink verified the effectiveness of the controller. In addition, a test platform of the EMVA for hardware-in-the-loop (HIL) simulation was established and the practicability of EMVA application to engine intake systems was validated preliminarily.

KEY WORDS : Electromagnetic valve actuators, Cylinder air charge, Control-oriented model, Torque control, Speed control

NOMENCLATURE

A_{eff} : effective flow area of the orifice (m^2)
c_d : discharge coefficient
D : cylinder diameter (m)
H_u : fuel heating value (kJ/kg)
i : number of sampling cycle
I : moment of inertia ($kg \cdot m^2$)
k : the ratio of the specific heats for air
k_p : proportional coefficient
L : intake valve lift (mm)
m_c : desired cylinder air charge (kg)
$\hat{m}_c$: simulation cylinder air charge (Kg)
$\dot{m}_c$: air mass flow into cylinder (kg/sec)
m_{fuel} : fuel mass (kg)
$\dot{m}_{fuel}$: fuel mass flow (kg/sec)
n : engine speed (rpm)
$\hat{n}$: simulation engine speed (rpm)
p_c : cylinder pressure during intake process (Pascal)
p_{up} : upstream pressure (Pascal)
P_i : indicated power (Watts)
R : gas constant
S : cylinder stroke (m)
T_c : cylinder air charge temperature (K)
T_{up} : upstream temperature (K)
T_i : indicated torque (N·m)
T_p : torque related to pumping losses (N·m)
T_f : torque related to frictional losses (N·m)
T_e : engine effective output torque (N·m)
$\hat{T}_e$: simulation engine effective output torque (N·m)
T_l : load torque (N·m)
T_D : differential time constant
T_I : integration time constant
V_c : cylinder volume (m^3)
Q_L : energy loss (J)
α : crank angle (degrees)
β : weight factor
ε : compression ratio
λ_s : crank radius-connecting rod length ratio
η_i : indicated efficiency
ω : angular speed (rad/sec)
$\hat{\omega}$: simulation crankshaft angular speed (rad/sec)
Δt : sampling period

1. INTRODUCTION

Traditional spark ignition engines use the throttle valve to regulate air mass flow which leads to pumping losses and cylinder air charge cannot respond rapidly to engine torque demand. The motion of the intake valves can be flexibly

*Corresponding author. e-mail: changsq@mail.njust.edu.cn

controlled by the introduction of electromagnetic valve actuators (EMVA). The engines equipped with EMVA can directly regulate the cylinder air charge with throttle plate wide opening. This results in reducing the pumping losses and increasing fuel economy by eliminating the need to throttle the air flow into the intake manifold. At the same time, such camless engines can eliminate the slow intake manifold filling dynamics which leads to faster breathing characteristics and can increase the engine transient torque performance (Ashhab *et al*., 2000; Venkatesh and Selvakumar, 2016).

To realize the advantage of EMVA, a controller of EMVA is necessary to regulate the motion of electromagnetic intake valves. The development of such controller requires a control-oriented model which can simulate the intake process under unthrottled operation. Mean value models of conventional engines with camshaft valvetrain concentrate on the intake manifold filling dynamics and express the air mass flow into cylinder by the speed-density equation (Guzzella and Onder, 2010). These models reflect the relationships among throttle angle, intake manifold pressure and cylinder air charge (Hendricks and Sorenson, 1990; Hendricks and Vesterholm, 1992; Hendricks *et al*., 1996). Therefore, they are not capable of simulating the intake process by regulating the motion of electromagnetic intake valves.

In order to model the effectiveness of the adjustment of the intake valve train on the intake process, a large number of researches have been done to improve the traditional mean value models. Ashhab *et al*. (1998) proposed a control-oriented model of unthrottled operations based on phenomenological models and experimental data, the relationship between cylinder air charge and the motion of intake valves was presented as look-up table in the model. The works by Wu *et al*. (2011) employed a filling-and-emptying model to simulate the air charge in the engines with variable valve train (VVT), which can simulate the changes in valve action. The works by Martensson and Flardh (2010) concentrated on modelling the effects of variable valve timing on volumetric efficiency and torque generation. Leroy *et al*. (2008, 2013) proposed an aspirated mass model for engines with variable-valve-actuation, the aspirated mass model consisted of three terms, i.e., classical speed-density equation used in traditional mean value models, the models of the impact of the gas exchange between intake and exhaust manifolds while overlap and the models of the impact of the residual gases. Compared with the works mentioned above, the flow through the intake valves in unthrottled intake process was treated as isentropic with isothermal conditions on the in-cylinder side in this study. The model proposed in this paper can reflect the relationship among engine output torque, cylinder air charge and the motion of electromagnetic intake valves. The previous studies on the fully flexible valve actuators mainly focused on the fields, such as the optimization and the control of the actuators hardware itself and research on the effects of the fully flexible valve actuators on the engine performance by one-dimensional simulations and experiment. These previous studies and this paper have different focuses. The study in this paper is an exploratory research on addressing the real-time control issue of a kind of the fully flexible valve actuators application which can realize the unthrottled engine operation.

This paper is the extension and improvement of a previous study (Chen *et al*., 2016). The model in the previous work only concentrated on simulating the torque generation and ignored the crankshaft rotational dynamics. In addition, the controller in the previous work just employed a feedforward module. The present paper is organized as follows. Section 2 introduces the development of the control-oriented model of camless engine. Based on

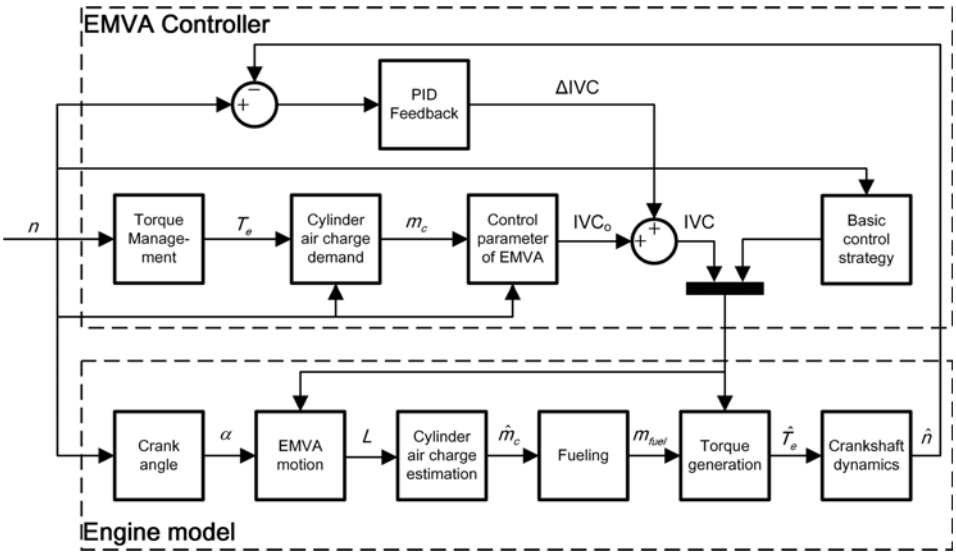

Figure 1. Block diagram of the model and the controller.

the model, the controller of EMVA which consists of a feedforward module and a PID feedback module is designed in Section 3. The controller's target is ensuring precise and rapid adjustment of the cylinder air charge by EMVA to maintain the engine demand. The simulations of engine speed control problems which is carried out in Matlab/Simulink to verify the effectiveness of the controller are described in Section 4. Figure 1 illustrates the structure of the model and controller in simulations, the details are presented in the following sections. An experimental platform for hardware-in-the-loop (HIL) simulation is introduced in Section 5, the HIL simulation results demonstrate the feasibility of the practical applications of EMVA to engine intake systems.

2. CONTROL-ORIENTED MODEL

2.1. Crank Angle

Crank angle α (degrees) can be specified as a function of engine speed and simulation time, which can be expressed as

$$\alpha = \int_0^t \frac{n(t)}{60} 360 \cdot dt \tag{1}$$

Where, n is engine speed (rpm).

2.2. EMVA Motion

This module simulates the motion of the electromagnetic intake valves according to the requirement of EMVA controller. Its output is the valve lift L in the crank angle domain and one of the inputs of the cylinder air charge estimation module. Figure 2 illustrates the examples of the intake valve profiles with different closing phases at engine speed of 2000 RPM.

2.3. Cylinder Air Charge Estimation

This module estimates the real-time cylinder air charge in each engine cycle. With throttle plate wide opening, the cylinder air charge is regulated by the intake valves, and it relates to the motion of intake valves and the cylinder pressure during intake process.

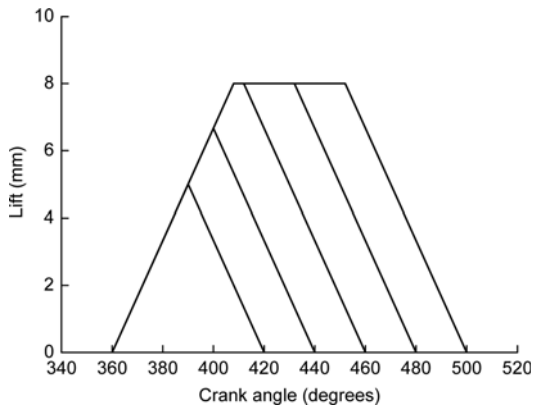

Figure 2. Intake valve profiles with different closing phases.

The air mass flow into cylinder $\dot{m}_c$ (kg/sec) is treated as isentropic and determined by upstream and downstream pressures of the intake valve. A quasi-steady model of flow through an orifice is used to describe the mass air flow into cylinder as shown in the following equation:

$$\dot{m}_c = c_d A_{eff} \frac{p_{up}}{\sqrt{RT_{up}}} \psi\left(\frac{p_c}{p_{up}}\right) \tag{2}$$

Where, c_d is discharge coefficient, A_{eff} is the effective flow area of the orifice (m^2), i.e., intake valve, p_{up} and T_{up} are upstream pressure (Pascal) and temperature (K), R is gas constant, p_c is the cylinder pressure during intake process (Pascal), and the function $\psi(x)$ is defined by

$$\psi(x) = \begin{cases} \sqrt{k\left(\frac{2}{k+1}\right)^{\frac{k+1}{k-1}}} & x < \left(\frac{2}{k+1}\right)^{\frac{k}{k-1}} \\ \sqrt{\frac{2k}{k-1}\left(x^{\frac{2}{k}} - x^{\frac{k+1}{k}}\right)} & x \geq \left(\frac{2}{k+1}\right)^{\frac{k}{k-1}} \end{cases} \tag{3}$$

and where, $k = 1.4$ is the ratio of the specific heats for air.

The downstream side, i.e., in-cylinder side, is considered as isothermal, the cylinder pressure during intake process p_c is derived from the ideal gas law and can be express as

$$\frac{dp_c}{dt} = \frac{1}{V_c}\left(RT_c\dot{m}_c - \frac{dV_c}{dt}p_c\right) \tag{4}$$

where, T_c is cylinder air charge temperature (K), V_c is the cylinder volume (m^3), and it can be expressed as a function of the crank angle as shown in the following equation

$$V_c = \frac{\pi}{8} SD^2 \left[\frac{2}{\varepsilon - 1} + 1 - \cos\alpha + \frac{1}{\lambda_s}\left(1 - \sqrt{1 - \lambda_s^2 \sin^2\alpha}\right)\right] \tag{5}$$

and where, S is cylinder stroke (m), D is cylinder diameter (m), ε is compression ratio, λ_s is crank radius-connecting rod length ratio.

In addition, discharge coefficient c_d is specified by a nonlinear function of intake valve lift L and obtained by experimental data. It is presented as a look-up table in the control-oriented model. c_d and A_{eff} are the parameters which reflect the relationship between intake valve motion and mass air flow into cylinder. With throttle plate wide opening, the change range of intake valve upstream pressure p_{up} is small and can be specified by a nonlinear function of engine speed and load in order to simplify the control-oriented model. According to the research by Zou (2006), comparing the mean value model with considering the changes in temperature in the intake process and that without considering the changes in temperature, the difference between the simulation results of air mass flow

is about 1 % ~ 2 %. At the same time, for simplifying the control-oriented model and joining the isentropic and isothermal processes, the values of T_{up} and T_c are considered equal and the air temperature changes in the intake process are ignored.

2.4. Fueling

For the sake of simplifying the model, the wall-wetting dynamics of the fuel film is ignored and the assumption that the air flow is uniform during intake process is employed. Then the fuel mass flow is derived according to the stoichiometric air-fuel mass ratio which is 14.67.

2.5. Torque Generation

The engine output effective torque is derived by using energy conservation law, it depends on indicated power, fictional losses and pumping losses. The indicated power P_i (Watts) can be expressed as

$$P_i = H_u \eta_i \dot{m}_{fuel} \tag{6}$$

where, H_u is fuel heating value (kJ/kg), η_i is indicated efficiency, and $\dot{m}_{fuel}$ is the fuel mass flow (kg/sec).

The indicated torque T_i (N·m) can be expressed as

$$T_i = \frac{30P_i}{\pi n} \tag{7}$$

The torque T_p (N·m) related to pumping losses can be expressed as

$$T_p = \frac{Q_L}{4\pi} \tag{8}$$

where, Q_L is the energy loss (J) that depends on the cylinder pressure differential between the intake and exhaust processes.

The torque T_f (N·m) related to frictional losses can be specified by a nonlinear function of the intake valve closing phase and engine speed in camless engine and obtained by experimental data. Based on the above mentioned, the engine effective output torque T_e (N·m) can be expressed as

$$T_e = T_i - T_p - T_f \tag{9}$$

In addition, the parameters η_i and Q_L can be specified by nonlinear functions of the intake valve closing phase and engine speed under unthrottled operation, and the functions are presented as maps in the model.

2.6. Crankshaft Rotational Dynamics

Crankshaft rotational dynamics can be expressed as

$$I\dot{\omega} = T_e - T_l \tag{10}$$

where, I is moment of inertia of the engine (kg·m^2), ω is angular speed (rad/sec), T_l is the external load torque (N·m).

3. CONTROLLER DESIGN

The controller employs a feedforward module and a PID feedback module, and its objective is ensuring that the cylinder air charge can fulfil the engine's torque demand and engine speed can track the speed reference by regulating the motion of the electromagnetic intake valves. In order to simplify the controller, the degrees of freedom of intake valves are reduced in different engine operating ranges which are partitioned based on engine speed and load, this is what we call basic control strategy.

3.1. Basic Control Strategy

The freedom degrees of the EMVA include valve lift, valve opening timing/phase, valve closing timing/phase (opening duration), opening/closing transition time and single/double intake valve mode. The increase of the freedom degrees can improve the engine performance, meanwhile, it increases the complexity of the controller and the difficulty of the development process. In order to simplify the controller, these parameters are reduced according to the basic idea that the controller regulates the air charge by controlling one motion parameter of those mentioned above at any particular engine operating conditions. In addition, the controller considers the single intake valve

Table 1. Partition of the engine operating ranges and corresponding fixed parameter values.

Operating ranges	Single/double mode	Maximum lift (mm)	Opening phase (degrees ATDC)	Opening and closing transition time (ms)
$1000 \le n < 2000$	Single	4	360	2
$2000 \le n \le 3000$	Single	8	360	4
$3000 < n \le 4000$ (Less than 70 % full engine load)	Single	8	360	4
$3000 < n \le 4000$ (More than 70 % full engine load)	Double	8	360	4
$4000 < n \le 5000$	Double	8	350	4
$5000 < n \le 6000$	Double	8	330	4

mode as the first choice comparing to the double mode by reason of reducing the power consumption of the actuators.

The cylinder charge motion can be enhanced by changing the motion of the intake valves which benefits the combustion, at the same time, the pumping losses are increasing. For achieving the balance of the conflict, a one-dimensional model of a prototype engine was established in AVL-Boost software environment, and the traditional intake valvetrain was replaced by the electromagnetic valve actuators in this model. Then the motion parameters of intake valves were optimized by simulation to approach the target which was making as intense cylinder charge flow as possible and as few pumping losses as possible (Xu *et al*., 2016). Based on the simulation results, the basic control strategy is determined that the controller regulates the cylinder air charge by adjusting the intake valve closing phase (IVC) and regards other parameters as different fixed values in different engine operating ranges. Table 1 shows the partition of the engine operating ranges and the corresponding fixed parameter values. Where, n is engine speed (rpm), and ATDC means After Top Dead Centre. This study concentrates on the operating ranges under engine speed of 3000 rpm.

3.2. Feedforward Control Scheme

Feedforward control scheme consists of torque management module, cylinder air charge demand module and control parameter of EMVA module. According to the basic control strategy, the feedforward controller chooses appropriate intake valve closing phase (IVC_o) to satisfy the engine torque demand, as shown in Figure 1.

3.2.1. Torque management

According to torque-based concept, the engine speed reference is translated into torque demand using optimizing control theory. This process is considered as torque management, and it decides the engine torque demand that the controller must track.

The torque management is regarded as optimal control issue, and its objective function is shown as

$$J = \int_{t_0}^{t_f} \left[\left(\hat{\omega}(t) - \omega(t) \right)^2 + \beta T_e^2(t) \right] dt \tag{11}$$

where, $\hat{\omega}$ is simulation crankshaft angular speed (rad/sec), ω is the angular speed reference (rad/sec), β is the weight factor. And its constraint is Equation (10).

For running simulation in computer, Equation (10) and (11) are rewritten to the following discretization form

$$\omega(i+1) = \omega(i) + \frac{\Delta t}{J_e} \left[T_e(i) - T_l(i) \right] \tag{12}$$

$$J = \sum_{i=0}^{k} \left[\left(\hat{\omega}(i) - \omega(i) \right)^2 + \beta T_e^2(i) \right] \cdot \Delta t \tag{13}$$

where, Δt is sampling period, and i is the number of sampling cycle.

This optimal control issue is considered as dynamic optimal problem and solved by using dynamic programming to derive the torque demand.

3.2.2. Cylinder air charge demand

The desired cylinder air charge m_c that the controller must track can be specified by a nonlinear function of engine speed and desired output torque. The nonlinear function is derived by experimental data and presented as a map in the controller.

3.2.3. Control parameter of EMVA

The relationships among the cylinder air charge, pumping losses, intake valve closing phases and engine speeds are investigated by simulations in the AVL-Boost software environment. Figure 3 illustrates the relationships between the cylinder air charge and intake valve closing phases at different engine speeds. As shown in Figure 3, the cylinder air charge is increasing as closing phase is increasing and it approximates a linear function. The air charge decreases when the closing phase increases beyond a value because of the air charge backflow from the cylinder. This closing phase value can be regarded as a saturation value and it is different at different engine speeds. Moreover, the valve actuators consume more power with longer opening

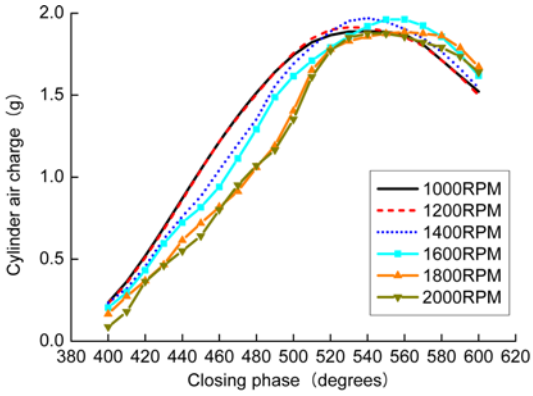

(a) 1000 to 2000 rpm with maximum lift of 4 mm

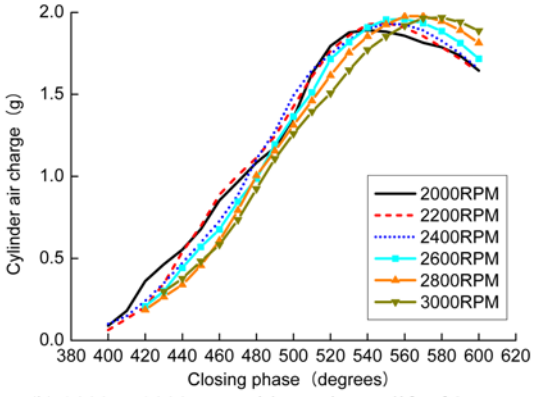

(b) 2000 to 3000 rpm with maximum lift of 8 mm

Figure 3. Relationships between cylinder air charge and intake valve closing phase at different engine speeds.

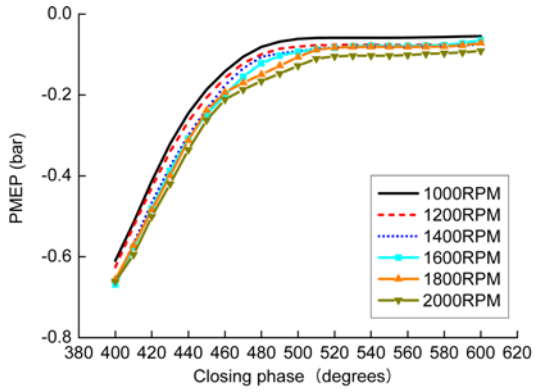

(a) 1000 to 2000 rpm with maximum lift of 4 mm

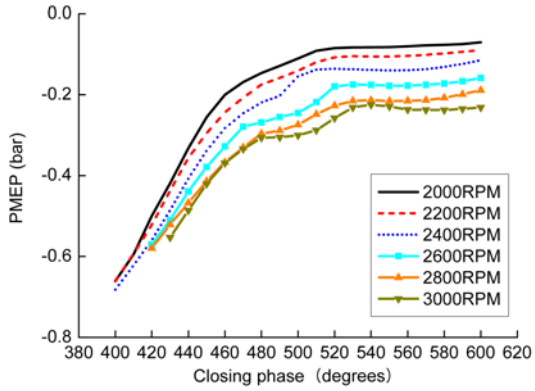

(b) 2000 to 3000 rpm with maximum lift of 8 mm

Figure 4. Relationships between pumping losses and intake valve closing phase at different engine speeds.

duration, thus, from the point of view of control design, there is no benefit from increasing the closing phase beyond the saturation value. This saturation value is considered as an upper bound for adjusting of the closing phase. In addition, as engine speed increases, valve opening duration in time domain with the same closing phase becomes shorter, and it has negative impact on cylinder air charge. When comparing Figure 3 (a) with (b), it is found that closing phase plays a more important role in cylinder air charge than maximum lift does.

Figure 4 illustrates the relationship of the pumping losses and intake valve closing phases at different engine speeds. The pumping losses can be expressed by pumping mean effective pressure (PMEP, bar) which is negative. As shown in Figure 4, PMEP is increasing with increasing closing phase and this is beneficial to output torque. There is also a saturation value of the closing phase, and PMEP does not increase and almost keeps invariant when the closing phase increases beyond this value. Because PMEP is a monotonically increasing function of the closing phase, the controller does not need to consider the influence of PMEP when adjusting the closing phase to regulate the cylinder air charge.

Based on the above mentioned, the relationships as shown in Figure 3 are considered as different maps corresponding to different engine operating ranges. The controller chooses appropriate motion parameters of the intake valves according to these maps and Table 1 under different engine working conditions.

3.3. PID Feedback Control Scheme

For the sake of compensating effort of the feedforward control scheme, the PID feedback controller was designed. It corrects the outputs of feedforward controller according to the deviations between the simulation engine speed and speed reference. As shown in Figure 1, it outputs the compensation value of the intake valve closing phase (ΔIVC). It can be expressed as

$$u_i = k_p\left[e_i + \frac{\Delta t}{T_I}\sum_{j=0}^{i} e_j + \frac{T_D}{\Delta t}(e_i - e_{i-1})\right] \tag{14}$$

$$e_i = \hat{n}(i) - n(i) \tag{15}$$

where, k_p is proportional coefficient, T_I is integration time constant, T_D is differential time constant, and $\hat{n}$ is the simulation engine speed (rpm).

4. SIMULATION RESULTS

The model and the controller depicted in Figure 1 were coded in Matlab/Simulink software environment, and the simulations of engine speed control problem were carried out to verify the effectiveness of the controller. The controller adjusts the motion of EMVA once per engine working cycle in the simulations.

4.1. Constant Speed Control

The controller's capability for constant speed control was tested in the condition that engine load changes suddenly. The controller's objective is ensuring that engine operates steadily at constant speed of 1500 rpm in this simulation, and the cycle of adjustment of EMVA is 0.08 s (engine working cycle at 1500 rpm).

As shown in Figure 5, a step change in load torque from 30 N·m to 50 N·m was applied at t = 0.50 sec. The controller adjusted the motion of EMVA for 5 times, at the time of 0.53 s, 0.61 s, 0.69 s, 0.77 s and 0.85 s respectively. In addition, in the period of 0.50 s to 0.53 s, the controller hasn't reacted to load change yet. However the load change resulted in the variation of engine speed, and engine speed change led to the variation of the parameter η_i (Equation 6), T_p (Equation 8) and T_f (Equation 9), that's why the simulation engine output torque varied in the time of 0.50 s to 0.53 s.

The controller approximately took 0.35 sec to stabilize the engine output torque and the engine speed. The fluctuation ranges of output torque and speed are about 20 N·m and 60 rpm (4 % of 1500 rpm), respectively. The simulation results demonstrate that the controller is capable of quickly stabilizing the engine operation at constant

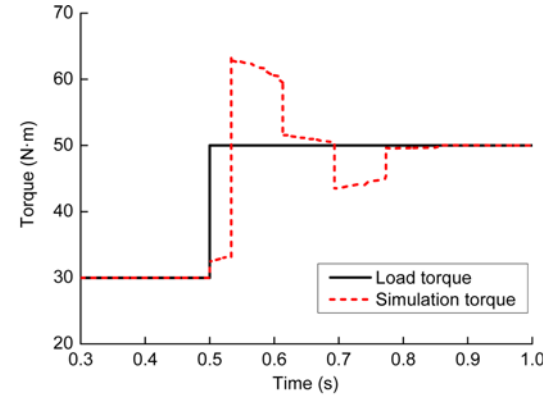

(a) Torque

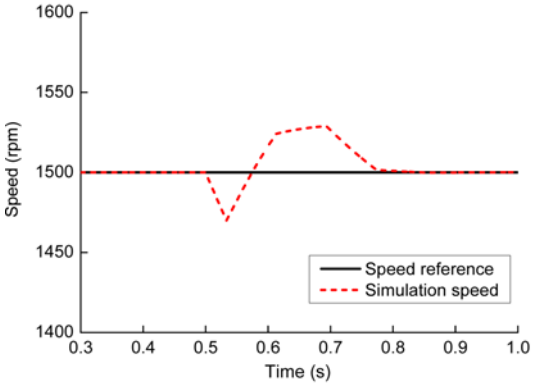

(b) Engine speed

Figure 5. Constant speed control simulation results.

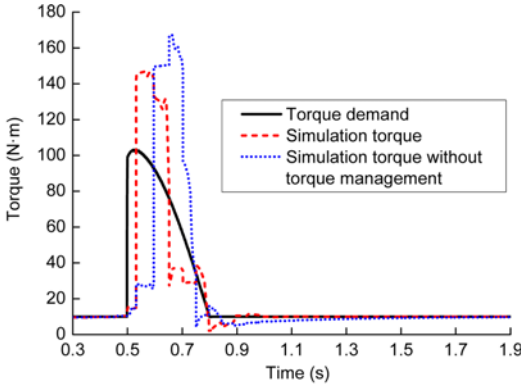

(a) Torque

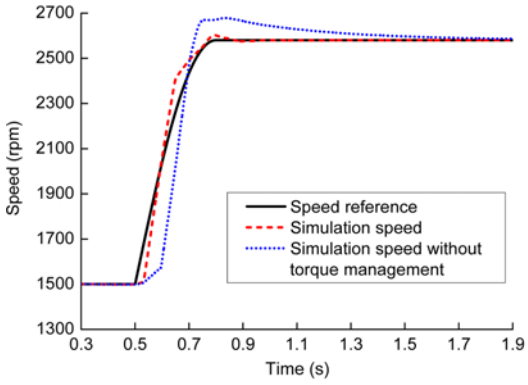

(b) Engine speed

Figure 6. Speed tracking control simulation results.

speed after a step change in load torque, with small fluctuation of output torque and engine speed.

4.2. Speed Tracking Control

In this simulation, the value of load torque was set to 10 N·m, and the reference speed increased from 1500 rpm to 2580 rpm in 0.30 sec with variable acceleration. Moreover, the simulation result with torque management was compared with that without torque management. The target of the controller is ensuring that engine operates in accordance with the speed reference.

As shown in Figure 6, the fluctuation of simulation torque with torque management is less than that without torque management. And the controller with torque management took about 0.35 sec to stabilize the engine speed and the overshoot is about 0.9 %. By contrast, the controller without torque management took approximately 2 secs to stabilize the speed and the overshoot is about 4 %. Moreover, the speed curve with torque management agrees better with the reference curve than that without torque management does. The simulation results verify the capability of the controller for speed tracking control.

Traditional engine commonly adjusts ignition advance angle and/or fuel injection to respond to the fast and transient speed and torque demand. For example, in the downshift process of automated mechanical transmission (AMT), engine speed needs to be increased within a short period for improving shift quality and shortening shift time. However, changing ignition advance angle has limited range of speed and torque adjustment, and changing fuel injection leads to the variation of air-fuel ratio which is detrimental to emission aftertreatment. EMVA provides an alternative approach to control the transient engine output which is the precise and quick adjustment of cylinder air charge. The simulation results shown in Figure 6 demonstrate the camless engine can regulate the output torque and speed quickly by controlling the motion of EMVA.

5. HIL SIMULATION

The EMVA presented in this paper is developed by our research group and based on the moving coil electromagnetic linear actuator (Chang *et al*., 2011; Liu and Chang, 2009). Compared with the electromagnetic valve with common double electromagnet structure, it has advantages in system response, valve seating performance and structure complexity. After several rounds of the development of prototypes, it basically meets the needs of practical application. The structure and hardware of EMVA are shown in Figure 7.

In engine equipped with EMVA, the EMVA controller

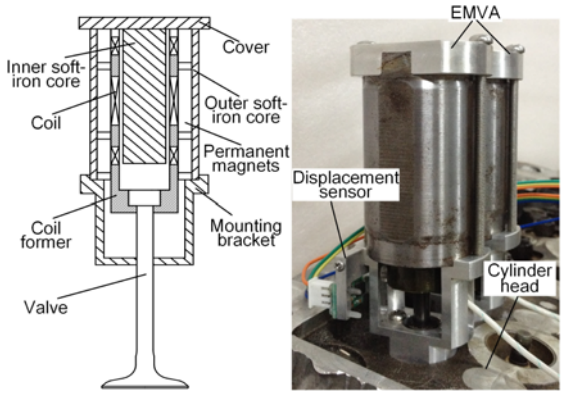

Figure 7. Structure and hardware of EMVA.

should be integrated in the engine ECU for high integration of the control system. According to engine speed and load, the controller calculates the EMVA motion parameters, including opening/closing phase, transition time and maximum lift, and then sends these parameters to the EMVA ECU through CAN Bus. The EMVA ECU realizes the motion as required.

The cylinder head of a four cylinder in-line engine was modified and the EMVA hardware was assembled on it, then the HIL simulation system of EMVA was constructed to verify the control system scheme mentioned above, based on dSPACE and DSP controller (model TMS320F2812). Figure 8 illustrates the structure of the system. The EMVA controller as shown in Figure 1 was running on DS1005 board of dSPACE, and DS4302 board of dSPACE communicated with DSP through CAN Bus and output EMVA motion parameters to DSP. According to the outputs of dSPACE, DSP controller, as the EMVA ECU, employs the backstepping sliding mode control method (Fan *et al*., 2016) and generates pulse width modulation (PWM) signals through drive circuit board to achieve the realization of the EMVA motion.

In the simulation, by varying engine speed n and desired torque T_e, the controller executed in dSPACE output different values of closing phases and maximum lift to examine if the real EMVA can work as the requirement of

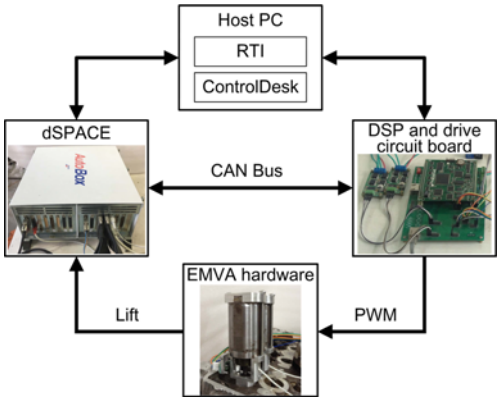

Figure 8. Structure of HIL simulation system.

Table 2. Parameters at 1500 rpm.

T_e (N·m)	Maximum lift (mm)	Opening phase (degrees)	Closing phase (degrees)
20	4	360	418.0
40	4	360	433.9
60	4	360	447.5
80	4	360	460.1
100	4	360	473.1
120	4	360	488.5
140	4	360	508.6

the controller. The values of T_e was set to increase from 20 N·m to 140 N·m with the step of 20 N·m at speeds of 1500 rpm and 2500 rpm. The parameters output from the controller are shown in Tables 2 and 3. The valve profiles collected by the displacement sensor are shown in Figures 9 and 10.

Compared Table 2 with Figure 9 and Table 3 with Figure 10, it is found that the actual closing phases lag behind for about 10 degrees. The major reason is that DSP reduces the valve seating velocity to achieve soft landing for the improvement of valve seating performance. The effect of

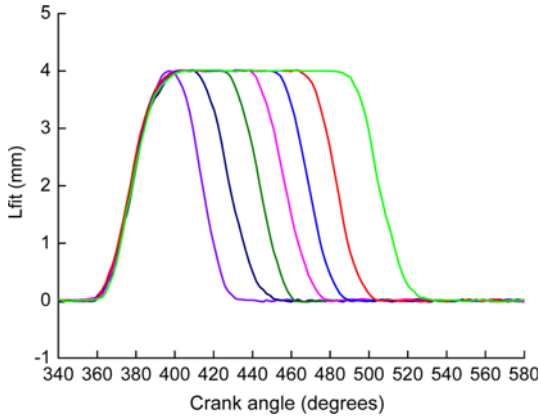

Figure 9. Valve profiles at 1500 rpm.

Table 3. Parameters at 2500 rpm.

T_e (N·m)	Maximum lift (mm)	Opening phase (degrees)	Closing phase (degrees)
20	8	360	440.3
40	8	360	455.6
60	8	360	468.9
80	8	360	481.4
100	8	360	494.2
120	8	360	508.3
140	8	360	524.2

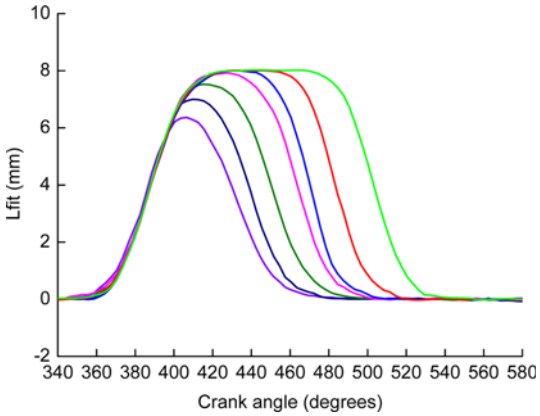

Figure 10. Valve profiles at 2500 rpm.

the lag on cylinder charge will be researched and the method of EMVA motion control will be improved in subsequent work.

The HIL simulation approximates the practical situation of EMVA working in the real engine intake system. The simulation results demonstrate that the EMVA hardware can work as requested by controller and verify the feasibility of the practical application of the EMVA to engine intake system.

6. CONCLUSION

The introduction of EMVA offers more design and control flexibility to engines. This paper concentrates on the control issue of the practical application of EMVA in engines, and conclusions can be obtained as follows.

(1) A control-oriented model of engine equipped with EMVA was developed which was capable of simulating the intake process in unthrottled condition.
(2) The EMVA controller was designed to regulate the motion of electromagnetic intake valves for ensuring that the cylinder air charge can fulfil the engine torque demand.
(3) The effectiveness of the EMVA controller was verified by the engine speed control simulations. The simulation results demonstrated that the controller was capable of controlling the engine output torque and speed by the precise and rapid adjustment of the cylinder air charge.
(4) The HIL simulation system has been established which approximated the working condition of EMVA in the real engine. The simulation results validated the practicability of the control system scheme and the application of the EMVA.

ACKNOWLEDGEMENT–The authors would like to appreciate the National Natural Science Foundation of China for their financial support (Grant No. 51306090).

REFERENCES

Ashhab, M. S., Stefanopoulou, A. G., Cook, J. A. and Levin, M. B. (1998). Camless engine control for a robust unthrottled operation. *SAE Paper No*. 981031.

Ashhab, M. S., Stefanopoulou, A. G., Cook, J. A. and Levin, M. B. (2000). Control-oriented model for camless intake process – Part I. *J. Dynamic Systems, Measurement, and Control* **122**, **1**, 122–130.

Chang, S., Liu, L., Li, Z. and Xu, Z. (2011). Application of engine electromagnetic actuated valvetrain. *J. Nanjing University of Science and Technology* **35**, **5**, 585–589.

Chen, H., Chang, S. and Fan, A. (2016). Control of intake process in an SI engine with electromagnetic valve actuator. *Proc. FISITA 2016*, BEXCO, Korea.

Fan, A., Chang, S. and Chen, H. (2016). Backstepping sliding mode control for an electro-magnetic valve actuator. *Proc. FISITA 2016*, BEXCO, Korea.

Guzzella, L. and Onder, C. H. (2010). *Introduction to Modeling and Control of Internal Combustion Engine Systems*. 2nd edn. Springer. Berlin, Germany, 32–35.

Hendricks, E., Chevalier, A., Jensen, M., Sorenson, S. C., Trumpy, D. and Asik, J. (1996). Modelling of the intake manifold filling dynamics. *SAE Paper No*. 960037.

Hendricks, E. and Sorenson, S. C. (1990). Mean value modelling of spark ignition engines. *SAE Paper No*. 900616.

Hendricks, E. and Vesterholm, T. (1992). The analysis of mean value SI engine models. *SAE Paper No*. 920682.

Leroy, T., Alix, G., Chauvin, J. and Le Berr, F. (2008). Modeling fresh air charge and residual gas fraction on a dual independent variable valve timing SI engine. *SAE Paper No*. 2008-01-0983.

Leroy, T. and Chauvin, J. (2013). Control-oriented aspirated masses model for variable-valve-actuation engines. *Control Engineering Practice* **21**, **12**, 1744–1755.

Liu, L. and Chang, S. (2009). Analysis and design of a moving-coil electromagnetic valve actuator. *Automotive Engineering* **31**, **8**, 733–766.

Martensson, J. and Flardh, O. (2010). Modeling the effect of variable cam phasing on volumetric efficiency, scavenging and torque generation. *SAE Paper No*. 2010-01-1190.

Venkatesh, D. and Selvakumar, A. (2016). A novel design of pneumatic actuator for camless engines. *SAE Paper No*. 2016-01-0099.

Wu, Y., Chen, B., Tsai, H. and Hsieh, F. (2011). New charging model using variable valve train for hil simulation. *SAE Paper No*. 2011-01-1150.

Xu, J., Chang, S., Fan, X. and Fan, A. (2016). Effects of electromagnetic intake valve train on gasoline engine intake charging. *Applied Thermal Engineering*, **96**, 708–715.

Zou, B. (2006). *Research on Model-based Air-fuel Ratio Control Technology of Gasoline Engine.* Ph. D. Dissertation. Zhejiang University. Hangzhou, China.